Expression and characterization of the biofilm-related and carnosine-hydrolyzing aminoacylhistidine dipeptidase from *Vibrio alginolyticus*

Ting-Yi Wang*, Yi-Chin Chen*, Liang-Wei Kao, Chin-Yuan Chang, Yu-Kuo Wang, Yen-Hsi Liu, Jen-Min Feng and Tung-Kung Wu

Department of Biological Science and Technology, National Chiao Tung University, Hsin-Chu, Taiwan, China

Correspondence

T.-K. Wu, Department of Biological Science and Technology, National Chiao Tung University, Hsin-Chu, Taiwan, China
Fax: +886 3 5725700
Tel: +886 3 5729287
E-mail: tkwmll@mail.nctu.edu.tw

*These authors contributed equally to this work

The biofilm-related and carnosine-hydrolyzing aminoacylhistidine dipeptidase (*pepD*) gene from *Vibrio alginolyticus* was cloned and sequenced. The recombinant PepD protein was produced and biochemically characterized and the putative active-site residues responsible for metal binding and catalysis were identified. The recombinant enzyme, which was identified as a homodimeric dipeptidase in solution, exhibited broad substrate specificity for Xaa-His and His-Xaa dipeptides, with the highest activity for the His-His dipeptide. Sequence and structural homologies suggest that the enzyme is a member of the metal-dependent metallopeptidase family. Indeed, the purified enzyme contains two zinc ions per monomer. Reconstitution of His·Tag-cleaved native apo-PepD with various metal ions indicated that enzymatic activity could be optimally restored when Zn^{2+} was replaced with other divalent metal ions, including Mn^{2+}, Co^{2+}, Ni^{2+}, Cu^{2+} and Cd^{2+}, and partially restored when Zn^{2+} was replaced with Mg^{2+}. Structural homology modeling of PepD also revealed a 'catalytic domain' and a 'lid domain' similar to those of the *Lactobacillus delbrueckii* PepV protein. Mutational analysis of the putative active-site residues supported the involvement of His80, Asp119, Glu150, Asp173 and His461 in metal binding and Asp82 and Glu149 in catalysis. In addition, individual substitution of Glu149 and Glu150 with aspartic acid resulted in the partial retention of enzymatic activity, indicating a functional role for these residues on the catalysis and zinc ions, respectively. These effects may be necessary either for the activation of the catalytic water molecule or for the stabilization of the substrate–enzyme tetrahedral intermediate. Taken together, these results may facilitate the design of PepD inhibitors for application in antimicrobial treatment and antibody-directed enzyme prodrug therapy.

Vibrio alginolyticus is one of twelve recognized marine *Vibrio* species that have been identified as pathogenic for humans and marine animals. This species causes infection in shrimps, fish, shellfish and squids, as well as in humans who are infected via consumption of undercooked seafood or exposure of wounds to warm seawater in coastal areas [1–3]. *V. alginolyticus* infects grouper culture by forming a biofilm in the intestine and causes fish mortality due to gastroenteritis syndrome [4]. A disease outbreak of shrimp farming in 1996 was also attributed to *V. alginolyticus* virulence [5]. In infected humans, clinical symptoms include gastroenteritis, wound infections and septicemia [6–8] and, more rarely, ear infections, chronic diarrhea exclusively in AIDS patients, conjunctivitis and post-traumatic intracranial infection [9–11]. Thus, prevention, early

detection and treatment of *V. alginolyticus* infections are important to maintain human and marine animal safety.

Dipeptidases play a general role in the final breakdown of peptide fragments produced by other peptidases during the protein degradation process [12]. Aminoacylhistidine dipeptidase (EC 3.4.13.3; also Xaa-His dipeptidase, carnosinase and PepD) catalyzes the cleavage and release of an N-terminal amino acid, which is usually a neutral or hydrophobic residue, from a Xaa-His dipeptide or degraded peptide fragment [13]. The PepD enzyme occurs extensively among prokaryotes and eukaryotes and belongs to the metallopeptidase family M20 from the metallopeptidase H (MH) clan (MEROPS: the Peptidase Database; http://merops.sanger.ac.uk/) [14,15]. This enzyme was generally identified as a dipeptidase with broad substrate specificity. Other proteins have been reported to have dipeptidase activity on unusual dipeptide carnosine (β-Ala-L-His) and homocarnosine (γ-amino-butyl-His) as well as on a few distinct tripeptides [13,16,17]. Other functional enzymes from the M20 family include aminoacylase-1 [18], *Pseudomonas* sp. carboxypeptidase G2 (CPG2) [19–21], *Saccharomyces cerevisiae* carboxypeptidase Y [19], bacterial PepT and PepV [15,20,21], *Escherichia coli* PepD [22], human nonspecific dipeptidase and human brain-specific carnosinase [16]. These enzymes have been implicated in cleavage of the final peptide fragments for amino acid utilization [13]. These enzymes have shown potential for application as an anti-bacterial target or a therapeutic agent for cancer treatment [21] and may possibly play roles in aging as well as neurodegenerative or psychiatric diseases [16].

Biofilm formation has been found in a wide variety of microbial infections within the body or on the surface of the host. Bacterial adhesion and subsequent biofilm formation stimulate the expression of biofilm-specific genes [23,24]. Alternatively, expression of *pepD* may negatively affect biofilm formation in *E. coli* [25]. *V. alginolyticus* may form a biofilm in the intestines of infected fish [4]. Although several members of M20 family enzymes have been studied extensively, the functional residues of PepD-related enzymes are poorly understood. To determine the importance of PepD in affecting biofilm formation and serving as a potential target for antimicrobial agents, we examined the *V. alginolyticus* PepD protein. In the present study, we present the cloning and expression of the *V. alginolyticus pepD* gene, the purification and biochemical characterization of the produced PepD recombinant protein, as well as a detailed analysis of its substrate specificity and the effects of metals on enzymatic activ-

ity and kinetic parameters. We also identified the putative amino acid residues responsible for catalysis and metal binding based on multiple sequence alignment and homology modeling from the related M20 family enzymes.

Results and Discussion

Cloning, sequence analysis and identification of the *V. alginolyticus pepD* gene

To clone the *pepD* gene from *V. alginolyticus*, we first aligned and analyzed multiple nucleic acid sequences of putative *pepD* genes from various *Vibrio* species to find highly conserved sequences. A DNA fragment of approximately 1.5 kb was amplified by PCR using *V. alginolyticus* ATCC 17749 genomic DNA as a template. Following confirmation of both the N- and C-terminus sequence of the *pepD* gene, an ORF that contained 1473 nucleotides and coded for a polypeptide of 490 amino acids was identified (Fig. 1). Sequence analysis predicted a protein with a molecular mass of 53.6 kDa and an isoelectric point of pH 4.7.

Production of the *V. alginolyticus* PepD protein

The *V. alginolyticus pepD* gene was then subcloned into the expression plasmid pET28a(+) and subsequently transformed into *E. coli* BL21(DE3)(pLysS) cells to generate the pET28a(+)-pepD recombinant plasmid for protein over-expression. Following isopropyl thio-β-D-galactoside induction for 6 h at 37 °C, the produced protein was harvested for protein purification using a Ni Sepharose™ 6 Fast Flow column and eluted with imidazole. SDS/PAGE of the homogeneous protein revealed a molecular mass of approximately 54 kDa (Fig. 2, lane 3) in agreement with the predicted molecular mass of 53.6 kDa. Immunoblot analysis with PepD monoclonal antibody also produced a single band (Fig. 2, lane 4). By contrast, the molecular mass of native PepD was 100.7 ± 6.0 kDa as determined by analytical sedimentation velocity ultracentrifugation (Fig. 3A), whereas this technique revealed a molecular mass of 51 kDa for the denatured PepD (Fig. 3B). These results indicate that the PepD protein associates as a homodimer in solution.

Biochemical characterization of *V. alginolyticus* PepD

The pH and temperature optima for purified recombinant PepD carnosine hydrolysis, substrate specific-

```
      gtgtctgagttccattctgaaatcagtaccttatcacctgctccactttggcagtttttc   60
1     M  S  E  F  H  S  E  I  S  T  L  S  P  A  P  L  W  Q  F  F
      gataagatttgttcaatccctcacccttcaaaacatgaagaagctctagcacagtacatt   120
21    D  K  I  C  S  I  P  H  P  S  K  H  E  E  A  L  A  Q  Y  I
      gttacttgggcaacagagcaaggttttgacgtacgccgcgatccaactggcaacgtgttc   180
41    V  T  W  A  T  E  Q  G  F  D  V  R  R  D  P  T  G  N  V  F
      attaaaaaacctgcgacaccaggtatggaaaacaaaaaaggtgtagtgcttcaagcacac   240
61    I  K  K  P  A  T  P  G  M  E  N  K  K  G  V  V  L  Q  A  [H]
      atcgacatggtgccacaaaagaacgaagacactgatcacgacttcactcaagatccaatt   300
81    I  [D]  M  V  P  Q  K  N  E  D  T  D  H  D  F  T  Q  D  P  I
      cagccatacatcgatggtgaatgggtaacagcaaagggcacaacgctaggtgcagataac   360
101   Q  P  Y  I  D  G  E  W  V  T  A  K  G  T  T  L  G  A  [D]  N
      ggcatcggcatggcttcttgtcttgctgtacttgcttctaaagagatcaagcacggtcct   420
121   G  I  G  M  A  S  C  L  A  V  L  A  S  K  E  I  K  H  G  P
      attgaagtttactgactattgatgaagaagcaggcatgacaggtgcatttggtcttgaa   480
141   I  E  V  L  L  T  I  D  [E]  [E]  A  G  M  T  G  A  F  G  L  E
      gctggctggttgaaaggcgatatccttctaaatacagactcagaacaagaaggcgaagtg   540
161   A  G  W  L  K  G  D  I  L  L  N  T  [D]  S  E  Q  E  G  E  V
      tacatgggttgtgcaggaggtatcgatggcgcaatgaccttcgatattactcgtgacgca   600
181   Y  M  G  C  A  G  G  I  D  G  A  M  T  F  D  I  T  R  D  A
      attccagcgggctttattactcgtcaactaacactgaaaggtctaaaaggcggtcactct   660
201   I  P  A  G  F  I  T  R  Q  L  T  L  K  G  L  K  G  G  [H]  S
      ggctgtgacatccatacaggtcgcggtaacgcaaacaaactgattggtcgcttcctcgct   720
221   G  C  D  I  H  T  G  R  G  N  A  N  K  L  I  G  R  F  L  A
      ggtcacgcgcaagagttggatcttcgcctggttgaattccgtggcggtagtttgcgtaac   780
241   G  H  A  Q  E  L  D  L  R  L  V  E  F  R  G  G  S  L  R  N
      gcgattcctcgtgaagcttttgtaactgtagcactaccggcagaaaatcaagataaacta   840
261   A  I  P  R  E  A  F  V  T  V  A  L  P  A  E  N  Q  D  K  L
      gcggaactgttcaactactacactgagttactaaaaacagagcttggtaaaattgaaaca   900
281   A  E  L  F  N  Y  Y  T  E  L  L  K  T  E  L  G  K  I  E  T
      gacatcgtgactttcaacgaagaagttgcaacagatgcacaagtgtttgcgattgcagac   960
301   D  I  V  T  F  N  E  E  V  A  T  D  A  Q  V  F  A  [I  A  D]
      caacaacgtttcatcgcagcattgaacgcttgtccaaacggtgtaatgcgtatgagtgat   1020
321   [Q  Q  R  F  I  A  A  L  N  A  C  P  N  G  V  M  R  M  S  D]
      gaagttgaaggcgtggttgaaacatcacttaacgttggtgttatcacaacagaagagaac   1080
341   [E  V  E  G  V  V  E  T  S  L  N  V  G  V  I  T  T  E  E  N]
      aaagtaaccgttctatgcctaattcgttccctgatcgactcaggtcgtagccaagttgaa   1140
361   [K  V  T  V  L  C  L  I  R  S  L  I  D  S  G  R  S  Q  V  E]
      ggtatgcttcaatctgtcgctgaactggctggtgctcaaattgaattctctggcgcttac   1200
381   [G  M  L  Q  S  V  A  E  L  A  G  A  Q  I  E  F  S]  G  A  Y
      ccaggctggaaaccagatgctgattcagagatcatggcaattttccgtgatatgtacgaa   1260
401   P  G  W  K  P  D  A  D  S  E  I  M  A  I  F  R  D  M  Y  E
      ggcatctacggtcacaagccaaacatcatggttatccacgcaggtcttgaatgtggtctg   1320
421   G  I  Y  G  H  K  P  N  I  M  V  I  H  A  G  L  E  C  G  L
      ttcaaagaaccttacccgaacatggatatggtttctttcggtccaaccatcaagttccct   1380
441   F  K  E  P  Y  P  N  M  D  M  V  S  F  G  P  T  I  K  F  P
      cattctccagatgagaaagtgaagatcgataccgttcaactgttctgggaccaaatggtt   1440
461   [H]  S  P  D  E  K  V  K  I  D  T  V  Q  L  F  W  D  Q  M  V
      gcgcttcttgaagccattcctgaaaaggcgtaa                               1473
481   A  L  L  E  A  I  P  E  K  A  -
```

■ (yellow) Metal-binding sites
■ (blue) Substrate-binding sites
■ (brown) Dimerization domain

Fig. 1. Nucleotide and predicted amino acid sequences of the *V. alginolyticus pepD* gene. His80, Asp119, Glu150, Asp173 and His461 (yellow) are putative metal ion-binding residues. Asp82, Glu149 and His219 (aquamarine) are putative catalytic residues. The Ile318–Ser397 residues (brown) encompass the expected dimerization domain.
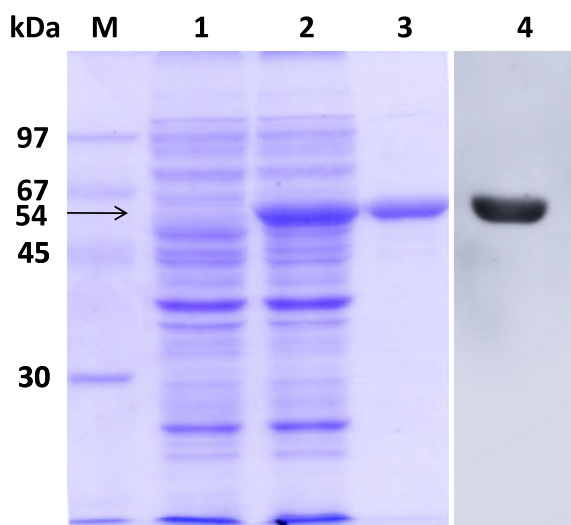
Fig. 2. SDS/PAGE and western blot analysis of purified *V. alginolyticus* PepD protein. Lane M, marker proteins: phosphorylase *b* (97 kDa), bovine serum albumin (67 kDa), ovalbumin (45 kDa) and carbonic anhydrase (30 kDa); lane 1, crude cell extracts of *E. coli* BL21(DE3)pLysS carrying pET-28a(+) plasmid; lane 2, crude cell extracts of *E. coli* BL21(DE3)pLysS carrying pET-28a(+)-pepD plasmid; lane 3, purified PepD from Ni-nitrilotriacetic acid column; lane 4, western blot analysis of purified PepD with monoclonal anti-PepD serum.

Fig. 3. Analytical ultracentrifugation of PepD protein. (A) The calculated molecular mass of native PepD from sedimentation coefficient (*s*) is approximately 100 664.94 ± 295 $g \cdot mol^{-1}$. (B) The calculated molecular mass of urea denatured PepD protein from sedimentation coefficient (*s*) is approximately 51 091.49 ± 113 $g \cdot mol^{-1}$.

ity, kinetic parameters, inhibition by a selection of protease inhibitors and the effects of metal ions were determined. The PepD activity was tested at various pH values using citric acid (pH 4, 5 and 6) and Tris–HCl (pH 6, 7, 7.4, 8.5, 9 and 9.5) (Fig. 4A). The pH activity of PepD showed an optimal activity in the range pH 7–7.4 and declined at more acidic and alkaline pH values. PepD retained only 80% and 86% of its maximal activity at pH 6 and 8.5, respectively. The PepD activity temperature curve was rather broad, with a range between 25–50 °C and maximum activity at 37 °C (Fig. 4B). Thus, PepD activity assays were performed at pH 7.4 and 37 °C.

The PepD from *E. coli* has been identified as a dipeptidase with broad substrate specificity [22]. The substrate specificity of *V. alginolyticus* PepD was determined with seventeen peptides, including eleven Xaa-His dipeptides, four His-Xaa dipeptides and two His-containing tripeptides at pH 7.4 and 37 °C (Fig. 5). The enzymatic activity on L-carnosine (β-Ala-L-His) was defined as 100%. The enzymatic activity was superior to that on L-carnosine for several Xaa-His dipeptides, including α-Ala-His, Val-His, Leu-His, Ile-His, Tyr-His, Ser-His and His-His, and two His-Xaa dipeptides, namely His-Asp and His-Arg. Interest-
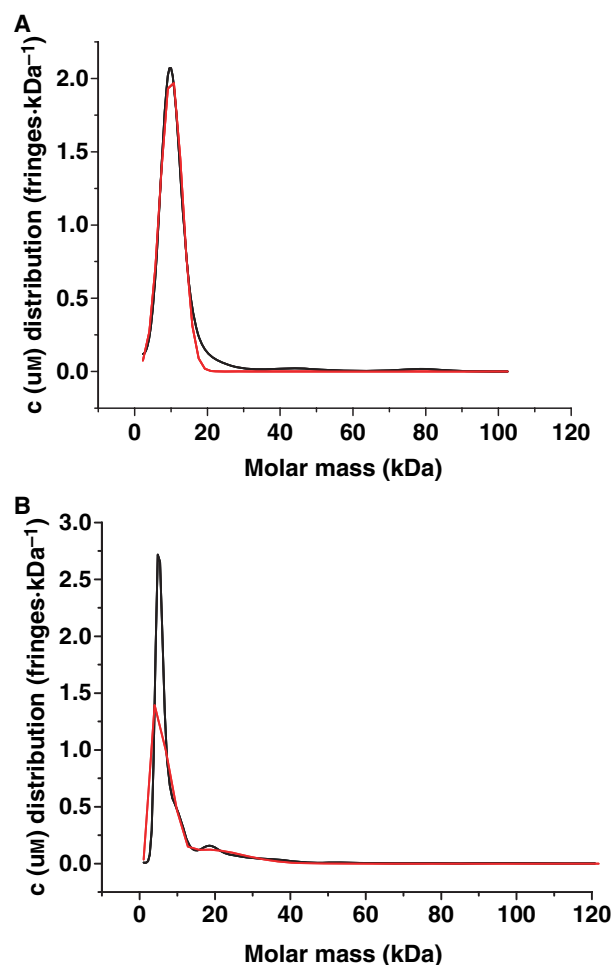
ingly, PepD exhibited its highest activity with the His-His dipeptide, and this activity was approximately two-fold higher than that with L-carnosine. Similarly, a preference for α-Ala-His compared to L-carnosine was first identified for bacterial PepD, although the same result has been observed in human cytosolic non-specific dipeptidase CN2 [16]. The enzyme exhibited decreased activity toward Gly-His (70%). PepD did not degrade β-Asp-L-His dipeptide, His-Ile dipeptide, His-Val dipeptide or the Gly-His-Gly and Gly-Gly-His tripeptides. These results indicate that the *V. alginolyticus* PepD is a Xaa-His dipeptidase with broad substrate specificities and that the enzymatic activity of PepD on Xaa-His dipeptide is dependent on the charge
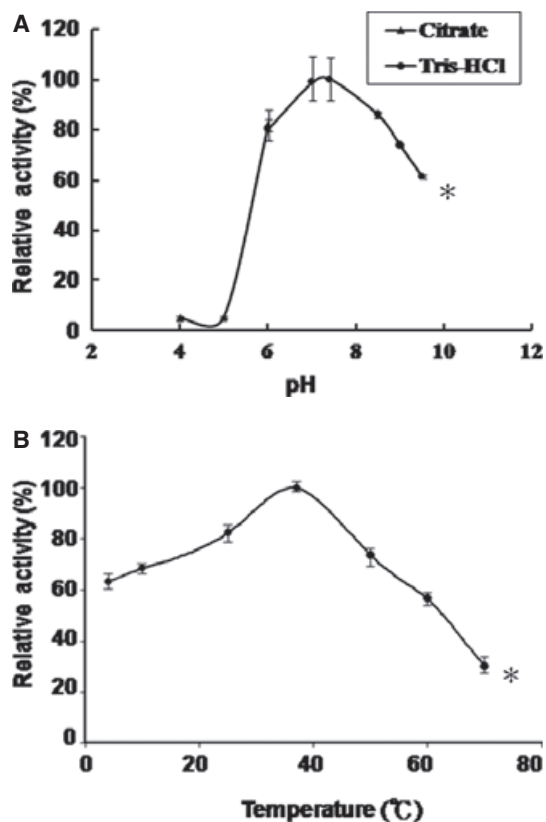
Fig. 5. Substrate specificity of PepD for Xaa-His, His-Xaa and His-containing tripeptides. Purified recombinant PepD proteins were incubated for 20 min at 37 °C with one of 11 Xaa-His dipeptides, four His-Xaa dipeptides and two His-containing tripeptides. The enzymatic activity was then measured using the standard activity assay. Values are expressed as relative activity compared to the hydrolysis of L-carnosine, which was set to 100%. *Statistical significance compared to the corresponding group ($P < 0.05$).

Fig. 4. (A) pH dependence of *V. alginolyticus* PepD activity. Citrate (pH 4.0, 5.0 and 6.0) and Tris–HCl (pH 6.0, 7.0, 7.4, 8.5, 9 and 9.5) buffer systems were used. (B) Temperature optimum of *V. alginolyticus* PepD. The enzyme was pre-incubated at 4, 10, 25, 37, 50, 60 and 70 °C for 30 min followed by analysis of the residual activity. The activity was expressed as a percentage of control activity determined under standard assay conditions. All reactions were carried out in triplicate and standard errors are shown. The activity at pH 7.4 and 37 °C was defined as 100%. *Statistical significance was determined by calculating the overall effect ($P < 0.05$).

of the N-terminus amino acid side chain because an amino group in the α or β position of the N-terminus residue did not affect the recognition and hydrolysis of the dipeptide. In addition, PepD is similar to the human nonspecific carnosinase CN2, which cannot hydrolyze the brain-specific dipeptide GABA-His (homocarnosine), and is different from PepV due to its inability to degrade unusual tripeptides.

PepD was capable of hydrolyzing the unusual dipeptide L-carnosine to β-alanine and L-histidine. Carnosine is assumed to act as a physiologically important buffer of zinc ions and prevent zinc-mediated injury. Additionally, L-carnosine exhibits antioxidant or cytoprotective properties [26]; acts as a cytosolic buffer [25], an antioxidant [27] and an antiglycation agent [28];
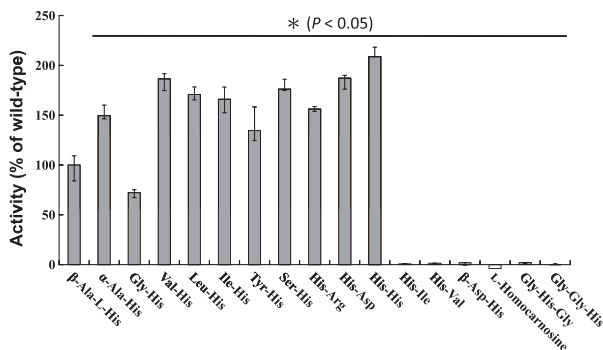
and inhibits DNA-protein cross-linking in neurodegenerative disorders such as Alzheimer's disease, in cardiovascular ischemic damage, and in inflammatory diseases [29]. Moreover, during bacterial infections, the degradation of L-carnosine via carnosinase or PepD-like enzymes may even enhance the destructive potential of bacteria, resulting in a pathological impact [12].

Kinetics and inhibition studies of *V. alginolyticus* PepD

For kinetic determinations, the apparent V_{max} and K_m values of *V. alginolyticus* PepD activity on L-carnosine were determined to be 1.6 μM·min^{-1} and 0.36 ± 0.07 mM, respectively. The turnover number (k_{cat}) and catalytic efficiency (k_{cat}/K_m) of *V. alginolyticus* PepD were 0.143 ± 0.02 s^{-1} and 0.398 ± 0.04 mM^{-1}·s^{-1}, respectively. Compared to human carnosinase (CN1) ($K_m = 1.2$ mM and $k_{cat}/K_m = 8.6$ mM^{-1}·s^{-1}), PepD catalysis occurs with a relatively low efficiency [16]. By contrast, the K_m value of *V. alginolyticus* PepD was lower than that of *E. coli* K-12 PepD (2–5 mM), and this finding indicates a relatively greater interaction of *V. alginolyticus* PepD with its substrates [22].

To classify the catalytic function of *V. alginolyticus* PepD, four common peptidase inhibitors were examined: benzamidine for serine endopeptidase, *N*-ethylmaleimide for cysteine endopeptidase, the metal-chelating agent EDTA, and bestatin for metalloenzymes. As expected, *V. alginolyticus* PepD activity was strongly inhibited by both EDTA and bestatin. Conversely, both benzamidine and *N*-ethylmaleimide

exhibited no apparent inhibitory effect on PepD activity at low concentrations. Bestatin has been reported to inhibit aminopeptidase B (K_I = 60 nM), leucine aminopeptidase (K_I = 20 nM) and aminopeptidase M (K_I = 410 nM, slow binding) but not aminopeptidase A, carboxypeptidase or endopeptidases. In the present study, bestatin inhibited PepD with a K_I of 37 nM. Therefore, *V. alginolyticus* PepD was identified as a metallopeptidase.

Effects of metal ions on *V. alginolyticus* PepD activity

The recombinant PepD fusion protein carried a His·Tag and a thrombin cleavage site in tandem as 5′-fusion partners. The 5′-fusion was removed by thrombin incubation and the native PepD protein was used for metal ion determination. The benzamidine-Sepharose column purified native PepD protein was subjected to inductively coupled plasma-MS and X-ray atomic absorption spectrum determination. These analyses demonstrated that PepD contains zinc as the divalent metal ion. We then investigated the effect of metal ion substitutions on the enzymatic activity of the native PepD protein. The native apo-PepD was dialyzed against a buffer containing EDTA to remove divalent metal ions and yield the inactive protein. Activation of native apo-PepD was then measured by incubating the protein with 2.5 equivalents or various concentrations of Mg^{2+}, Mn^{2+}, Co^{2+}, Ni^{2+}, Cu^{2+} and Cd^{2+} (Fig. 6). Optimal activation of apo-PepD was observed with various divalent metal ions, including Mn^{2+}, Co^{2+}, Ni^{2+}, Cu^{2+} and Cd^{2+}. Addition of Co^{2+} ions to native apo-PepD increased the enzyme activity by a factor of approximately 1.4 compared to the wild-type native PepD containing zinc. Moreover, Zn^{2+} did not inhibit Co^{+2}-loaded PepD activity. Substitution of Zn^{2+} with Mg^{2+} resulted in an approximate 80% restoration of the optimal enzymatic activity.

Bioinformatic analysis and homology modeling of *V. alginolyticus* PepD

Bioinformatics analysis of the *V. alginolyticus* PepD protein revealed high sequence homology to that of other *Vibrio* spp. (94–76% identity) and other bacteria (75–63%). Further analysis of PepD revealed a consensus sequence of nine amino acid residues, [170](NTDAEGRL)-N(T/V)D(S/T/G)E(E/Q/D)(I/N/E)G[178]-, similar to that found in PepA and members of this family [17]. In addition, sequence analysis revealed no putative signal peptide sequence, consistent with the observation that the PepD decoded from *V. alginolyticus* 12G01 may be an intracellular enzyme. On the other hand, sequence-based alignments of PepD with proteins of known peptidase clan MH structures, such as *Aeromonas* (*Vibrio*) *proteolyticus* aminopeptidase [14], *Streptomyces griseus* aminopeptidase S [30], CPG2 [31], *Salmonella typhimurium* PepT [32], human aminoacylase-1 (hAcy1) [33] and *Lactobacillus delbrueckii* PepV [12], showed low sequence identities in the range 7–20% and low sequence similarities in the range 13–34%.

Despite the lack of detectable sequence homology, putative active-site residues for catalysis were relatively conserved in PepD and related di-zinc enzymes in the M20 family [12,31]. His80, Asp119, Glu150, Asp173 and His461 were predicted to be involved in metal binding, whereas Asp82 and Glu149 were predicted to be necessary for catalysis. These residues were completely conserved, except for Asp173. Asp173 was present in homologs with aminopeptidase/dipeptidase specificity, whereas members of aminoacylase/carboxypeptidase contained a glutamic acid in the same position. To examine the overall structural features and the spatial locations of the putative active-site residues of the *V. alginolyticus* PepD, a homology model of PepD was obtained using *L. delbrueckii* PepV as the template despite poor amino acid sequence identity (20% identity) between the two sequences. PepV belongs to the MEROPS M20 metalloprotease family and contains a di-zinc binding domain and a small domain that is inserted in the middle of the metal-binding domain and mediates catalysis. The di-zinc
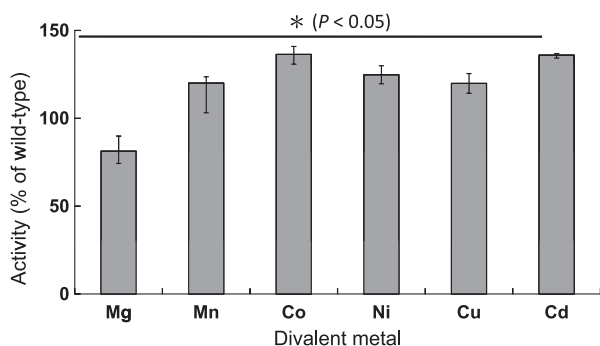

Fig. 6. Metal effects on the enzymatic activity of *V. alginolyticus* native PepD protein. The activity assays were performed at 37 °C for 30 min in the presence of 50 mM Tris–HCl buffer (pH 7.4), 2 mM L-carnosine, 10 μM of purified enzyme and 25 μM of the different metal salts. The activity was measured according to the standard activity assay protocol. Values are expressed as relative activity based on setting the hydrolysis of L-carnosine to 100%. Standard errors are shown (*n* = 3). *Statistical significance compared to the corresponding group (*P* < 0.05).

binding domain is a characteristic feature of the MH clan of co-catalytic zinc peptidases [12,31]. Structural homology modeling revealed that both proteins are highly homologous in 3D structures, which are putatively composed of a catalytic domain and a lid domain that interact with each other (Fig. 7A). This structural homology revealed that the putative metal-binding residues are almost superimposed on each

Fig. 7. Structural homology modeling of *V. alginolyticus* PepD. (A) 3D crystal structure of PepV (left) and the generated PepD model (right) based on the PepV monomer structure. The structure predicts two zinc ions in the catalytic pocket, and these ions are held by five metal-binding residues (yellow), including the adjacent residue Asp119 (light green). The residues for catalysis (blue) were quite similar between the two enzymes. (B) Local view of PepD superimposed with the active-site residues of PepV and CPG2. The active-site residues are indicated by gray, yellow and cyan for PepD, PepV and CPG2, respectively. The active-site residues are almost equivalent. The zinc-binding residue Asp173 in PepD and the equivalent aspartic acid in PepV were substituted by glutamic acid in CPG2.

other, except for the Asp119 residue, which is likely to be the residue that holds both zinc ions in PepV (Fig. 7B). The conserved Asp119 of PepD aligned with Asp120 in PepV. This residue is adjacent to its metal binding residue Asp119, whereas an Ala118 residue within PepD is located at the corresponding position to PepV Asp119. The lid domain also contains a fold similar to that of PepV. The C-terminal region was predicted to fold back into the catalytic domain to form a cavity and is probably involved in substrate specificity. Furthermore, the section of the PepD lid domain located between residues 318 and 397 exhibited sequence and structural homology to the dimerization domain of CPG2. PepV, an enzyme in the M20 family with a known structure, was identified as a monomer, whereas CPG2 exists as a homodimer in the native state [12,31]. Whether the dimerization domain in PepD is involved in catalysis is unclear, although the dimerization domain of CPG2 was reportedly similar to the lid domain of PepV according to a database search [12].
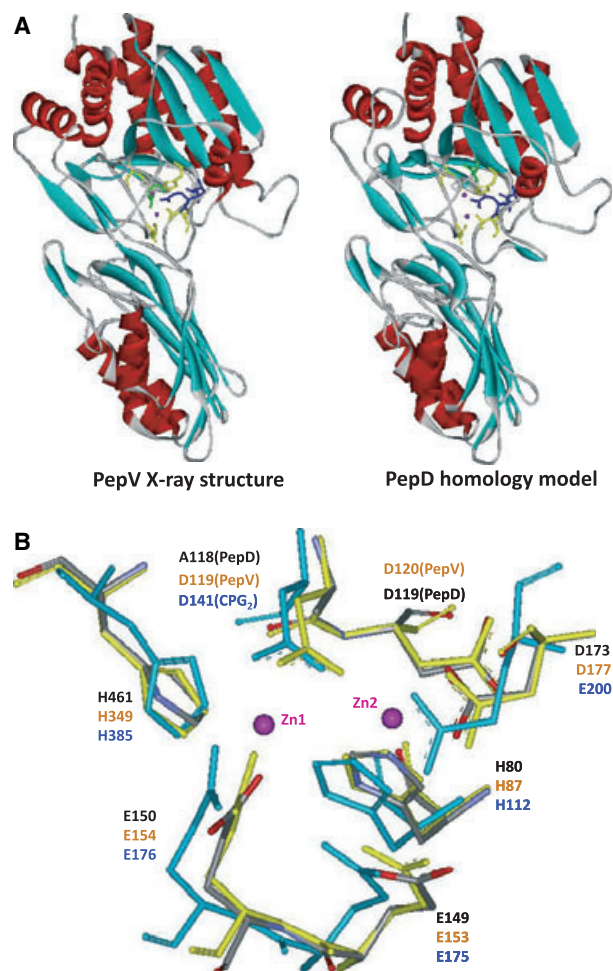
Site-directed mutagenesis of *V. alginolyticus* PepD

To assess the importance of both putative metal-binding sites in the dinuclear zinc center of PepD, each of these residues (His80, Asp119, Glu150, Asp173 and His461) was mutated individually using alanine-scanning mutagenesis. The mutated PepD proteins were produced similarly to the wild-type PepD. All mutants exhibited similar purification characteristics and the same electrophoretic mobility as the wild-type enzyme in SDS/PAGE. Although each of the mutations produced similar quantities of the protein, no activity was detected. Similar mutagenesis studies of hAcy1, which is classified in the same family as PepD, also led to a 10^3- to 10^5-fold decrease in enzymatic activity [33]. These results indicate the importance of these residues in the stability of di-zinc binding and suggest that these residues are essential for the enzymatic activity of the PepD.

To investigate whether site-directed mutagenesis of the amino acid residues provokes conformational changes that inactivate the enzymatic activity, CD spectrum analysis was performed to determine the secondary structure content of the purified PepD wild-type and mutant proteins. Loss of enzymatic activity in the mutants was not due to changes in the secondary structure of the proteins because the CD spectra of the PepD wild-type and mutants were similar. Determination of the apparent molecular masses by analytical sedimentation velocity ultracentrifugation showed

that the H80A mutant was expressed as an inclusion body, whereas both D82A and D119A were mainly monomers and D149A, D150A, D173A and H461A were homodimers (data not shown).

We then investigated the residues putatively involved in catalysis. Thus, Asp82 and Glu149 were substituted with amino acids with similar or different properties. PepD Asp82 is two residues downstream from His80 in the vicinity of the zinc center and is assumed to clamp the imidazolium ring of His80. Glu149 is in the immediate vicinity of the Glu150 of the zinc center and is assumed to act as a general base during catalysis to accept a proton from the zinc-bound water molecule. Asp82 was substituted with Gly, Val, Phe, Tyr, His and Glu, whereas the Glu149 was replaced with Gly, Ala, Ile, Ser, His, Trp and Asp. As expected, no activity was detected for any of the Asp82 mutants. Surprisingly, although most of the Glu149 mutants lost their enzymatic activity, the Glu149Asp mutant exhibited approximately 55% of the wild-type activity. Moreover, enzyme kinetics study showed that the apparent K_m, V_{max} and K_{cat}/K_m of the Glu149Asp mutant were 0.53 mM, 1.1 μM·min^{-1} and 0.186 mM^{-1}·s^{-1}, respectively.

Three of the putative metal-binding residues, Asp119, Glu150 and Asp173, were also subjected to further characterization by site-directed mutagenesis and enzymatic activity assay due to their putative discrepancies in metal binding. In PepV, Asp119 was predicted to be the bridging residue and to simultaneously hold both zinc ions. The structural homology model revealed that the side-chain ligands were disposed with two zinc ions (Zn1 and Zn2). The Zn1 is coordinated by the Nε2 of His80, one of the carboxylate oxygens of the bridging Asp119, and the carboxylate oxygen of Asp173. This model also showed that Zn2 is coordinated by the other carboxylate oxygen of the bridging Asp119, the carboxylate oxygen of Glu150, and the His461 Nε2. In addition, a 'bridging' water molecule was predicted between both zinc ions and close to the carboxylate group of the catalytic Glu149. The zinc-binding Asp173 in PepD was identified as in PepV, *Aeromonas* (*Vibrio*) *proteolyticus* aminopeptidase, *S. griseus* aminopeptidase S and PepT, whereas a glutamic acid was present at the equivalent site in CPG2 and hAcy1.

Asp119 was substituted with Glu, Met, Leu, Ile, Arg, Phe, Ala, Ser, Thr, Cys, Pro and Asn. As expected, substitution of Asp119 with other proteinogenic amino acid residues completely abolished enzymatic activity. On the other hand, substitution of Glu150 with Asp retained approximately 60% of the maximal hydrolytic activity of the wild-type enzyme, whereas substitution of Glu150 to Arg or His completely abolished enzymatic activity. Perhaps the replacement of Glu with Asp at this position only partially affects the metal ligand-binding affinity and subsequent activation of the catalytic water for substrate–enzyme tetrahedral intermediate formation. This effect, in turn, resulted in only partial loss of the enzymatic activity. Finally, substitution of Asp173 to Glu also completely abolished the enzymatic activity. This finding is consistent with the observation reported by Lindner *et al.* [33] that all homologs with proven aminopeptidase or dipeptidase specificity contain an aspartic acid, whereas a glutamic acid residue was identified in the same position in Acyl1/M20 family members that exhibit either aminoacylase or carboxypeptidase specificity. Thus, the lack of enzymatic activity for the Asp173Glu mutant may account for the discrepancy of the substrate specificity between the aminopeptidase/dipeptidase and aminoacylase/carboxypeptidase groups of the M20 family enzymes.

Hydrolytic mechanism of *V. alginolyticus* PepD

The high level of conservation of the active-site residues between *V. alginolyticus* PepD and related di-zinc peptidases indicates that the hydrolytic mechanism are likely closely related in all co-catalytic metallopeptidases from the MH clan. In support of this conclusion, the putative active-site residues involved in metal binding and catalysis in *V. alginolyticus* PepD were found to superimpose well with those in all six available structures from the MH clan. A general mechanism for PepD, which is similar to that of PepV, may be described (Fig. 8): (a) a fixed 'bridging' water molecule in PepD is predicted to be between both zinc ions and close to the carboxylate group of the catalytic Glu149; (b) upon substrate binding, the water molecule will be positioned between both zinc ions and the carbonyl carbon of the scissile peptide bond; (c) an attacking hydroxyl ion nucleophile is subsequently generated through the activation of the water molecule by both the zinc ions and transfer of the proton to the Glu149; (d) the carbonyl oxygen will be bound in an 'oxyanion-binding hole' formed by Zn1 and the imidazole group of His219 in PepD (corresponding to H269 in PepV), resulting in the polarization of the carbonyl group and facilitating the nucleophilic attack of the scissile bond by the zinc-oriented hydroxyl group; and (e) this leads to a tetrahedral intermediate, which subsequently decays to the product after one additional proton transfer from the catalytic Glu149 carboxylate to the amide nitrogen in His219.

On the other hand, although the results from our mutational analysis of PepD generally corroborate the
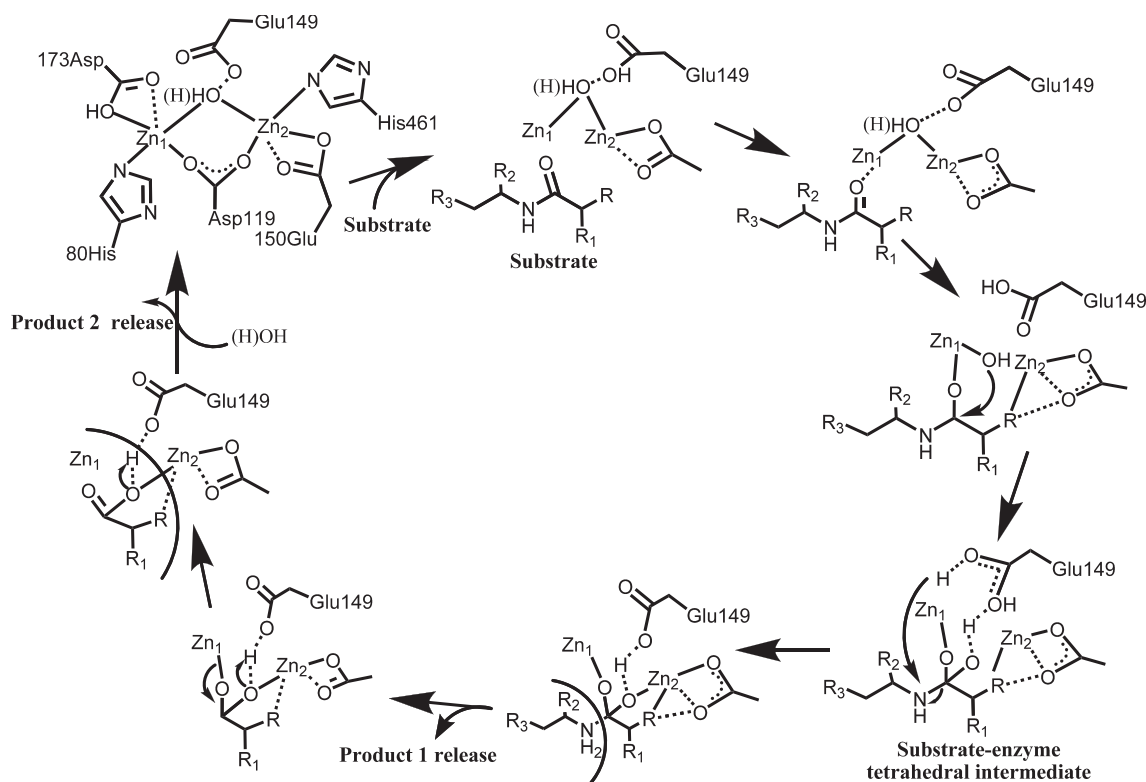
Fig. 8. The proposed general mechanism for PepD-catalyzed dipeptide hydrolysis. This metallopeptidase contains a co-catalytic active site where R1, R2 and R3 are substrate side chains and R is an N-terminal amine or a C-terminal carboxylate.

catalytic significance of a fully intact active-site domain, replacement of Glu149 or Glu150 with the one carbon shorter aspartic acid having the same negative charge retained partial enzymatic activity. Because the bridging catalytic water attacks the carbonyl carbon of the scissile peptide bond to form a sp³-orbital substrate–enzyme tetrahedral intermediate, the electrostatic and steric effects between the catalytic water and the carbonyl carbon of the Glu149 changed when substituted with other amino acid residues. Perhaps the substitution of the putative glutamic acid to the aspartic residue partially hinders the water molecule from activation to generate a hydroxyl ion nucleophile for subsequent tetrahedral intermediate formation. This substitution may also have enlarged the active-site cavity and reduced substrate binding affinity or substrate–enzyme tetrahedral intermediate formation and, thus, resulted in the partial loss of enzymatic activity. Alternatively, the Glu149Asp substitution may partially affect the metal-binding affinity of the adjacent Glu150 residue, and this alteration may then impede the functional role of the zinc ions, either for activation of the catalytic water molecule or stabilization of the substrate–enzyme tetrahedral intermediate. Previ-

ously, Lindner *et al.* [33,34] reported that substitution of the general base Glu147 in hACy1 with Asp resulted in complete loss of enzymatic activity. These authors suggested that substitution of Glu with Asp altered the appropriate position for activation of the catalytic water and moved the residue close to Asp348 with the same charge. The introduction of unfavorable interactions between the two residues would cause the complete loss of enzymatic activity. Perhaps a structural but not a catalytic role between both enzymes may account for the discrepancy of enzymatic activity because both low sequence identity and slight differences in the 3D structure of the active-site cavity between the enzymes were noticed (data not shown). For the Glu150Asp mutation, shortening the amino acid side chain in this position might reduce the metal-binding affinity, which, in turn, would hinder the substrate–enzyme tetrahedral intermediate formation and cause partial loss of enzymatic activity.

Interestingly, the results of these studies indicate that the enzymatic activity of the native apo-PepD enzyme may be activated optimally by excess amounts of Mn^{2+}, Co^{2+}, Ni^{2+}, Cu^{2+} and Cd^{2+}, and weakly by Mg^{2+}. Notably, the postulated role of the metal atoms

is the stabilization of the bridging water molecule with the resulting formation of a hydroxide ion [34]. Perhaps the overall structure of PepD is essentially unchanged upon binding of various metal ions at the active site, and only small variations in the bond lengths to the ligand side chains occur. Consistent with this hypothesis, both Mg^{2+} and Mn^{2+} atoms bind to the active site of APPro in a very similar manner; however, Mn^{2+} activates APPro, whereas Mg^{2+} does not [35]. The arrangement of ligands at the active site of apo-PepD that are ideal for transition metal ions but less than optimal for Mg^{2+} may contribute to the weak binding of Mg^{2+} and enzymatic activity because proteins and enzymes generally bind Mg^{2+} weakly [36]. Nevertheless, understanding the differences in binding and enzymatic activity due to binding of various metal ions by active-site residues requires further investigation.

In summary, a PepD protein from *V. alginolyticus* was successfully produced, and active-site residues putatively involved in metal binding and catalysis were identified. The striking structural similarity between PepD and the related di-nuclear metalloproteases strongly suggests that these enzymes may have the same evolutionary origin and have divergently evolved to exhibit different peptidase specificities. Site-directed mutagenesis of the putative active-site residues to other proteinogenic amino acid residues resulted in the complete loss of enzymatic activity, except for the Glu149Asp and the Glu150Asp mutations. The substitution of the glutamic acid to the aspartic acid with the same negative charge but one less carbon atom may enlarge the active site cavity and reduce the substrate–enzyme or enzyme–metal ion interactions and, consequently, alter the enzymatic activity. Finally, due to the potential function of carnosine in buffering zinc ions and in enhancing the destructive potential during bacterial infection, the characterization of PepD will have a significant impact on both our fundamental scientific understanding and the biotechnological application of this type of enzymes. Further studies aiming to elucidate the physiological and structural characteristics of PepD and related M20 family enzymes and probe the discrepancies of different substrate specificities are warranted.

Experimental procedures

Bacterial strains and materials

The *V. alginolyticus* strain (ATCC 17749) was obtained in a freeze-dried form from the Culture Collection and Research Center (CCRC, Hsin-Chu, Taiwan). The QIA-amp DNA Mini Kit was obtained from Qiagen (Hilden, Germany). Protein molecular weight standards and a protein assay kit were obtained from Bio-Rad (Hercules, CA, USA).

Cloning and DNA sequencing of the *V. alginolyticus pepD* gene

Multiple nucleic acid sequences of PepD from *Vibrio parahaemolyticus* RIMD 2210633 (BA000031), *Vibrio vulnificus* YJ016 (BA000037) and *Vibrio cholerae* O1 biovar eltor str. N16961 (AE004299) were aligned and analyzed with CLUSTALW (http://www.ebi.ac.uk/clustalw) to identify conserved sequences among *Vibrio* spp. *pepD* genes. Based on the highly conserved 5′- and 3′-end nucleic acid sequences of the *Vibrio* spp. *pepD*, we designed a set of primers (F1: 5′-GTGTCTGAGTTCCATTC-3′ and R1: 5′-TTACGCCTTTTCAGGAA-3′) to obtain the *V. alginolyticus pepD* gene. The *V. alginolyticus* genomic DNA was extracted using the Qiagen QIAamp DNA Mini Kit according to the manufacturer's protocol. The *V. alginolyticus pepD* gene was obtained via PCR using *V. alginolyticus* genomic DNA as the template. The reaction was carried out under the following conditions: denaturation at 94 °C for 2 min followed by 29 cycles of denaturation at 94 °C for 4 s, annealing at 56 °C for 1 min, and extension at 72 °C for 2 min followed by a final extension at 72 °C for 15 min. The resulting PCR product was subcloned into the pCR2.1®-TOPO vector (Invitrogen, Carlsbad, CA, USA) to construct the recombinant plasmid pCR2.1®-TOPO-pepD. The recombinant plasmid was subjected to restriction endonuclease digestion to confirm the presence of the insert and then sequenced. The dideoxy chain-termination method using an ABI PRISM BigDye Terminator v3.1 Cycle Sequencing Reaction kit and an Applied PRISM® 3100 Genetic Analyzer (Applied Biosystems, Foster City, CA, USA) was used to determine the sequences. In addition, both the N- and C-terminus sequences were verified with the synthesized internal sequence primers obtained from the core region sequence. The nucleotide sequence of the *V. alginolyticus pepD* gene has been deposited in the GenBank database (accession number DQ335448).

Production and purification of *V. alginolyticus* PepD recombinant protein

The *pepD* gene was subcloned into the expression plasmid pET28a(+) and this new plasmid was transformed into *E. coli* BL21(DE3)(pLysS) cells for PepD recombinant protein production and purification. Colonies grown on an LB plate were inoculated into LB broth supplemented with 50 μg·mL^{-1} kanamycin and grown at 37 °C until A_{600} of 0.5–0.6 was reached. At this point, protein production was induced by the addition of isopropyl thio-β-D-galactoside to a final concentration of 0.5 mM, and the culture was

incubated at 37 °C for an additional 6 h before harvest. The cells were harvested by centrifugation and then resuspended in 15 mL of 20 mM Tris–HCl (pH 7.6) buffer (Calbiochem, La Jolla, CA, USA). The mixture was sonicated, and the cell debris was removed by centrifugation at 12 000 *g* for 30 min at 4 °C.

The supernatant containing produced PepD was loaded on a Ni Sepharose™ 6 Fast Flow column (GE Healthcare, Uppsala, Sweden) previously washed with ten column volumes of buffer A (20 mM Tris–HCl, 0.5 M NaCl, pH 7.4) containing 20 mM imidazole. The protein-loaded column was washed with five column volumes of buffer A + 20 mM imidazole and then five column volumes of buffer A containing 40, 100, 200, 300 and 500 mM imidazole. Fractions of 1 mL were collected, and the protein concentration in each fraction was determined using the BCA Protein Assay Reagent (Pierce, Rockford, IL, USA) with BSA as the standard. Fractions containing PepD enzymatic activity were pooled and dialyzed twice against 2 L of 50 mM Tris–HCl (pH 7.4). The purified recombinant PepD proteins were stored at −80 °C for 6 months without a loss of activity.

For the characterization of metal ion effect, the 5′-fusion of His·Tag and thrombin cleavage site sequence was cleaved from recombinant PepD protein. The recombinant PepD protein was digested with thrombin for 16 h in 40 mM Tris–HCl (pH 8.0), 300 mM NaCl, 2 mM CaCl$_2$ and 5% glycerol. The protein solution was loaded on a benzamidine-Sepharose™ 6B column to remove thrombin (GE Healthcare). The flow through fractions were collected and subjected to a Ni Sepharose™ 6 Fast Flow column to remove His·Tag and the uncleaved recombinant PepD protein. The His·Tag-cleaved native PepD protein fractions were collected, pooled and dialyzed against 1 L of 50 mM Tris–HCl (pH 6.8). The native PepD proteins were stored at −80 °C until use.

V. alginolyticus PepD enzymatic activity assay

The PepD activity was assayed according to the method by Teufel *et al.* [16], which is based on the measurement of a histidine product by *O*-phthaldialdehyde (OPA) modification. Briefly, substrate hydrolysis was carried out in a final volume of 200 μL containing 80 μL of 50 mM Tris–HCl buffer (pH 7.4), 100 μL of 2 mM L-carnosine (dissolved in 50 mM Tris–HCl, pH 7.4) and 20 μL of purified enzyme (0.5 mg·mL^{-1}, ∼ 9 μM). The reaction was initiated by addition of substrate and stopped by addition of 50 μL of 1% trichloroacetic acid after a 30-min incubation at room temperature. Next, 50 μL of 5 mg·mL^{-1} OPA dissolved in 2 M NaOH was added to derivatize the liberated histidine, and the reaction was incubated for 15 min at 37 °C in darkness. The fluorescence of the OPA-derivatized L-histidine was measured using Fluoroskan Ascent FL (Thermo Scientific, Waltham, MA, USA) (λ_{Exc}: 355 nm and λ_{Em}: 460 nm).

Reactions with only L-histidine or only L-carnosine were treated in parallel to serve as the positive and negative controls, respectively. All reactions were carried out in triplicate.

Preparation of monoclonal antibody

A 0.5-mL solution, containing equal parts of Freund's complete adjuvant and Ni Sepharose™ 6 Fast Flow chromatography-purified PepD (100 μg), was injected into female BALB/c mice. After three booster injections consisting of 100 μg of protein, emulsified with Freund's incomplete adjuvant, at an interval of 10 days, the animals were bled for hybridization, 4 days after the last injection. The myeloma cell line (FO) was fused with spleen cells from immunized BALB/c mice, at a ratio of 1 : 5. The culture medium (obtained between days 14 and 21 after fusion) was assayed for the production of specific antibodies by a solid-phase ELISA, using purified protein as the respective antigen. The positive hybridomas were recloned by the limiting dilution method at least twice. The cloned hybridoma cells were injected into the peritoneum of BALB/c mice pretreated with 0.5 mL of Freund's incomplete adjuvant and, approximately 2 weeks later, ascetic fluid was collected. The specificity of the antibody was confirmed by western blotting.

Substrate specificity of *V. alginolyticus* PepD

Various Xaa-His dipeptides (100 μL, 2 mM), including β-Ala-L-His (L-carnosine), α-Ala-L-His, Gly-His, Val-His, Leu-His, Ile-His, Tyr-His, Ser-His, His-His, β-Asp-L-His and γ-amino-butyryl-His (GABA-His, homocarnosine), and four His-Xaa dipeptides (His-Ile, His-Val, His-Asp, His-Arg), as well as two histidine-containing tripeptides, Gly-Gly-His and Gly-His-Gly, were used to investigate the substrate specificity of PepD. The reaction solutions were incubated for 20 min at 37 °C, stopped by the addition of 50 μL of OPA solution, and analyzed spectrofluorimetrically, as described above. The activity on L-carnosine was defined as 100%.

pH optimum and thermostability

The optimal pH profile of PepD was determined at 37 °C in a final volume of 200 μL at various pH values in 50 mM citric acid (pH 4, 5 and 6) and 50 mM Tris–HCl (pH 6, 7, 7.4, 8.5, 9 and 9.5). The effect of temperature on the enzymatic activity was determined according to the previously described activity assay procedure carried out at various temperatures (4, 10, 25, 37, 50, 60 and 70 °C). The enzyme thermostability was determined by pre-incubation of the enzyme at various temperatures (4, 10, 25, 37, 42, 50, 60 and 70 °C) at pH 7.4 for 30 min before adding the substrate. The residual activity was measured as previously described.

Metal ion effect of PepD activity

The thrombin-cleaved native PepD protein was first dialyzed overnight in buffer containing 20 mM Mes (pH 6.0) and 5 mM EDTA to remove the zinc ions. The native apo-PepD was dialyzed twice with 20 mM Mes (pH 6.0) and exchanged with 20 mM Hepes (pH 7.0) before adding the various divalent metal ions. The apo-PepD protein concentration was adjusted to 0.01 mM before addition of metal ions. The following metal ions were used: $MgCl_2$, $MnCl_2$, $CoCl_2$, $NiCl_2$, $CuCl_2$, $ZnCl_2$ and $CdCl_2$. Various concentrations (2, 5, 10, 15, 20, 25, 50 and 100 μM) of divalent metal ions were used. The activity assay was performed as previously described. Inductively coupled plasma-MS analysis was performed on a Perkin Elmer SCIEX ELAN 5000 Inductively Coupled Plasma Mass Spectrometer (Perkin-Elmer, Boston, MA, USA). The X-ray atomic absorption spectrum was determined at the National Synchrotron Radiation Research Center (NSRRC, Hsin-Chu, Taiwan).

Analytical sedimentation velocity ultracentrifugation

An analytical ultracentrifugation method developed by Stafford [37] was applied to characterize the solution-state, especially the subunit stoichiometries, of the PepD protein. Briefly, 500 μL of the PepD protein equilibrated in 20 mM Tris–HCl (pH 6.8) buffer were subjected to analytical ultracentrifugation to obtain an apparent distribution of sedimentation coefficients (s) and the determined apparent molecular mass. In addition, 500 μL of buffer alone was used as the reference control in the reference sector.

Inhibition studies of the PepD activity

Several possible inhibitors, such as benzamidine, EDTA, bestatin and *N*-ethylmaleimide, were prepared as stock solutions in 50 mM Tris–HCl (pH 7.4). Inhibition assays were performed by pre-incubating different concentrations of the inhibitors with the enzyme for 30 min at 37 °C. Following this incubation, the enzymatic reaction was initiated by the addition of the substrate as described previously. IC_{50} values for the inhibitors were determined by PepD residual activity versus inhibitor concentration.

Enzyme kinetics of PepD

For determination of V_{max}, K_m and k_{cat} of *V. alginolyticus* PepD wild-type and mutants, the method described by Csámpai *et al.* [38] was slightly modified for use with HPLC and fluorescence detection [38]. Different concentrations of substrate (2.5, 5, 10, 25, 50, 100, 250, 500 μM and 1 mM) were added to nanomolar concentration of enzyme solution in 200 μL at pH 7.4 for 20 min at 37 °C. The liberated histidine was derivatized with 100 μL of OPA reagent for 5 min at 37 °C, and the fluorescence was detected as described previously. The substrate conversion did not exceed 20%. A total of nine substrate concentration points were used for each determination. The data collected were applied to the Lineweaver–Burk equation. The k_{cat}/K_m values reflect values assuming 100% activity of the enzyme preparation. All reactions were carried out in triplicate.

Sequence analysis of *V. alginolyticus* PepD

Protein translation was carried out using the EXPASY translation tool (http://ca.expasy.org/tools/dna.html). The molecular weight and theoretical pI of the protein were calculated by PROTPARAM (http://ca.expasy.org/tools/protparam.html). Homology searches of the DNA and amino acid sequences were performed using BLAST software (http://www.ncbi.nlm.nih.gov/blast). The alignments of DNA and protein sequences were performed with CLUSTALW (http://www.ebi.ac.uk/clustalw).

Site-directed mutagenesis of *pepD* gene

Site-directed mutagenesis of the *V. alginolyticus pepD* gene was performed using the QuikChange site-directed mutagenesis kit (Stratagene Inc., La Jolla, CA, USA). Mutagenic primers were designed (Table 1) and pET-28a(+)-pepD plasmid (wild-type) was used as the template. Mutations

Table 1. Mutagenic primers. Altered nucleotides are underlined.

Mutant	Predicted role in PepD	Oligonucleotide sequence (5′- to -3′)
H80A	Zinc binding	GTGCTTCAAGCAGCGATCGACATGGTGCCAC
D82A	Catalytic	GCACACATCGCCATGGTGCCACAAAAGAACG
D119A	Zinc binding	CGCTCGGGGCAGCTAACGGCATCGGCATGGC
D119X	Zinc binding	CGCTCGGGGCANNNAACGGCATCGGCATGGC
E149A	General base	CTGACGATCGATGCAGAAGCAGGCATGACAGG
E149X	General base	CTGACAATTGATNNNGAAGCAGGCATGACAGG
E150A	Zinc binding	ACTATTGATGAAGCCGCGGGCATGACAGGTGC
D173A	Zinc binding	CCTTCTAAATACAGCTAGCGAACAAGAAGGCG
H461A	Zinc binding	CCAACCATCAAGTTCCCTGCTAGCCCAGATGAG

were confirmed by DNA sequencing using the dideoxy chain-termination method and the ABI PRISM 3100 autosequencer (Applied Biosystems). The recombinant mutant plasmids were transformed into *E. coli* BL21(DE3) pLysS competent cells for production of the mutated PepD proteins.

References

1 Levine WC & Griffin PM (1993) Vibrio infections on the Gulf Coast: results of first year of regional surveillance. Gulf Coast Vibrio Working Group. *J Infect Dis* **167**, 479–483.

2 Marano NN, Daniels NA, Easton AN, McShan A, Ray B, Wells JG., Griffin PM & Angulo FJ (2000) A survey of stool culturing practices for vibrio species at clinical laboratories in Gulf Coast states. *J Clin Microbiol* **38**, 2267–2270.

3 Morris JG Jr & Black RE (1985) Cholera and other vibrioses in the United States. *N Engl J Med* **312**, 343–350.

4 Lee KK (1995) Pathogenesis studies on *Vibrio alginolyticus* in the grouper, *Epinephelus malabaricus*, Bloch et Schneider. *Microb Pathog* **19**, 39–48.

5 Lee KK, Yu SR, Chen FR, Yang TZ & Liu PC (1996) Virulence of *Vibrio alginolyticus* isolated from diseased tiger prawn *Penaeus monodon*. *Curr Microbiol* **32**, 229–231.

6 Blake PA, Weaver RE & Hollis DG. (1980) Diseases of humans (other than cholera) caused by vibrios. *Annu Rev Microbiol* **34**, 341–367.

7 Hlady WG. & Klontz KC (1996) The epidemiology of *Vibrio* infections in Florida, 1981–1993. *J Infect Dis* **173**, 1176–1183.

8 Rose JB, Epstein PR, Lipp EK, Sherman BH, Bernard SM & Patz JA (2001) Climate variability and change in the United States: potential impacts on water- and foodborne diseases caused by microbiologic agents. *Environ Health Perspect* **109**(Suppl. 2), 211–221.

9 Caccemese SM & Rastegar RD (1999) Chronic diarrhea associated with *Vibrio alginolyticus* in an immunocompromised patient. *Clin Infect Dis* **29**, 946–947.

10 Lessner AM, Webb RM & Rabin B (1985) *Vibrio alginolyticus* conjunctivitis. First reported case. *Arch Ophthalmol* **103**, 229–230.

11 Lipp EK, Huq A & Colwell RR (2002) Effects of global climate on infectious disease: the cholera model. *Clin Microbiol Rev* **15**, 757–770.

12 Jozic D, Bourenkow G, Bartunik H, Scholze H, Dive V, Henrich B, Huber R, Bode W & Maskos K (2002) Crystal structure of the dinuclear zinc aminopeptidase PepV from *Lactobacillus delbrueckii* unravels its preference for dipeptides. *Structure* **10**, 1097–1106.

13 Rawlings ND & Barrett AJ (1995) Evolutionary families of metallopeptidases. *Methods Enzymol* **248**, 183–228.

14 Chevrier B, Schalk C, D'Orchymont H, Rondeau JM, Moras D & Tarnus C (1994) Crystal structure of *Aeromonas proteolytica* aminopeptidase: a prototypical member of the co-catalytic zinc enzyme family. *Structure* **2**, 283–291.

15 Barrett AJ, Rawlings ND & Woessner JF (1998) Introduction: clan MH containing varied co-catalytic metallopeptidases. In *Handbook of Proteolytic Enzymes* (Barrett AJ, Rawlings ND & Woessner JF, eds), pp. 1412–1416. Academic Press, London.

16 Teufel M, Saudek V, Ledig JP, Bernhardt A, Boularand S, Carreau A, Cairns NJ, Carter C, Cowley DJ, Duverger D *et al.* (2003) Sequence identification and characterization of human carnosinase and a closely related non-specific dipeptidase. *J Biol Chem* **278**, 6521–6531.

17 Walker ND, McEwan NR & Wallace RJ (2005) A pepD-like peptidase from the ruminal bacterium, *Prevotella albensis*. *FEMS Microbiol Lett* **243**, 399–404.

18 Brenner DJ, Hickman-Brenner FW, Lee JV, Steigerwalt AG, Fanning GR, Hollis DG, Farmer JJ III, Weaver RE, Joseph SW & Seidler RJ (1983) *Vibrio furnissii* (formerly aerogenic biogroup of *Vibrio fluvialis*), a new species isolated from human feces and the environment. *J Clin Microbiol* **18**, 816–824.

19 Spormann DO, Heim J & Wolf DH (1992) Biogenesis of the yeast vacuole (lysosome). The precursor forms of the soluble hydrolase carboxypeptidase yscS are associated with the vacuolar membrane. *J Biol Chem* **267**, 8021–8029.

20 Vongerichten KF, Klein JR, Matern H & Plapp R (1994) Cloning and nucleotide sequence analysis of pepV, a carnosinase gene from *Lactobacillus delbrueckii* subsp. lactis DSM 7290, and partial characterization of the enzyme. *Microbiology* **140**, 2591–2600.

21 Hellendoorn MA, Franke-Fayard BM, Mierau I, Venema G. & Kok J (1997) Cloning and analysis of the pepV dipeptidase gene of *Lactococcus lactis* MG1363. *J Bacteriol* **179**, 3410–3415.

22 Schroeder U, Henrich B, Fink J & Plapp R (1994) Peptidase D of *Escherichia coli* K-12, a metallopeptidase of low substrate specificity. *FEMS Microbiol Lett* **123**, 153–159.

23 Alexander JB & Ingram GA (1992) Noncellular nonspecific defense mechanism of fish. *Annu Rev Fish Dis* **2**, 249–279.

24 Davies DG. & Geesey GG (1995) Regulation of the alginate biosynthesis gene algC in *Pseudomonas aeruginosa* during biofilm development in continuous culture. *Appl Environ Microbiol* **61**, 860–867.

25 Vaughan-Jones RD, Spitzer KW & Swietach P (2006) Spatial aspects of intracellular pH regulation in heart muscle. *Prog Biophys Mol Biol* **90**, 207–224.

26 Boldyrev AA (2000) Problems and perspectives in studying the biological role of carnosine. *Biochemistry (Mosc)* **65**, 751–756.

27 Decker EA, Livisay SA & Zhou S (2000) A re-evaluation of the antioxidant activity of purified carnosine. *Biochemistry (Mosc)* **65**, 766–770.

28 Seidler NW (2000) Carnosine prevents the glycation-induced changes in electrophoretic mobility of aspartate aminotransferase. *J Biochem Mol Toxicol* **14**, 215–220.

29 Guiotto A, Calderan A, Ruzza P & Borin G (2005) Carnosine and carnosine-related antioxidants: a review. *Curr Med Chem* **12**, 2293–2315.

30 Greenblatt HM, Almog O, Maras B, Spungin-Bialik A, Barra D, Blumberg S & Shoham G. (1997) *Streptomyces griseus* aminopeptidase: X-ray crystallographic structure at 1.75 Å resolution. *J Mol Biol* **265**, 620–636.

31 Rowsell S, Pauptit RA, Tucker AD, Melton RG, Blow DM & Brick P. (1997) Crystal structure of carboxypeptidase G2, a bacterial enzyme with applications in cancer therapy. *Structure* **5**, 337–347.

32 Hakansson K & Miller CG. (2002) Structure of peptidase T from *Salmonella typhimurium. Eur J Biochem* **269**, 443–450.

33 Lindner HA, Lunin VV, Alary A, Hecker R, Cygler M & Menard R (2003) Essential roles of zinc ligation and enzyme dimerization for catalysis in the aminoacylase-1/M20 family. *J Biol Chem* **278**, 44496–44504.

34 Lindner HA, Alary A, Boju LI, Sulea T & Menard R (2005) Roles of dimerization domain residues in binding and catalysis by aminoacylase-1. *Biochemistry* **44**, 15645–15651.

35 Graham SC, Bond CS, Freeman HC & Guss JM (2005) Structural and functional implications of metal ion selection in aminpopeptidase P, a metalloprotease with a dinuclear metal center. *Biochemistry* **44**, 13820–13836.

36 Cowan JA (2002) Structural and catalytic chemistry of magnesium-dependent enzymes. *Biometals* **15**, 225–235.

37 Stafford WF (1997) Sedimentation velocity spins a new weave for an old fabric. *Curr Opin Biotechnol* **8**, 14–24.

38 Csampai A, Kutlan D, Toth F & Molnar-Perl I (2004) o-Phthaldialdehyde derivatization of histidine: stoichiometry, stability and reaction mechanism. *J Chromatogr A* **1031**, 67–78.